TRIUMF	UNIVERSITY OF ALBERTA EDMONTON, ALBERTA	
	Date 2004/02/14	*File No.* TRI-DNA-04-2
Author GM Stinson		*Page* 1 *of* 15
Subject Beam transport from the medium β exit to beam transport to the ISAC-II experimental area		

1. Introduction

A recent note[1] has detailed a proposed system for beam transport to the experimental hall of ISAC-II. This report presents a possible beam-transport system from the exit of the medium β section of the accelerators to the object point for the beam transport of that reference.

We also include plots of the beam profiles from the medium β exit to each of the four target locations defined in ref[1].

2. Initial conditions

In this section we indicate the coordinate system used in this note and the initial phase-space parameters used in the optics calculations for the beamline presented here.

2.1 Coordinate system

In this report we use a Cartesian coordinate system, (z, x), with its origin at the intersection of a north-south line through the ISAC-I rfq and and east-west line through the ISAC-I DTLs. The positive z-axis points east and the positive x-axis points north.

In this coordinate system the location of the exit of the medium β section is given in ref[2] as $(z, x) = (26.101 \text{ m}, 19.000 \text{ m})$.

2.2 Initial phase space

Figure 8 of ref[2] is a plot of beam envelopes for the transport configuration suggested in that report. In particular, at the exit of the accelerator ref[2] gives the Twiss parameters

$$\alpha_x = \alpha_y = 0.10 \qquad \text{and} \qquad \beta_x = \beta_y = 1.70 \text{ m} .$$

Although these parameters have been calculated at the exit of the complete accelerator system, they should be reasonable approximations of what is to be expected at the exit of the medium β cavity[3]. Consequently, we use these values to calculate the value of the Twiss parameter γ as

$$\gamma_{x,y} = \frac{1+\alpha_{x,y}^2}{\beta_{x,y}} = \frac{1+(0.10)^2}{1.70} = 0.59412 .$$

To be consistent with the emittance used in ref[1], we use emittances of

$$\epsilon_x = \epsilon_y = 2\pi \text{ mm-mrad}$$

In the horizontal plane these values of α_x, β_x, γ_x, and ϵ_x correspond TRANSPORT input parameters of

$$\begin{aligned} x &= \sqrt{\beta_x \epsilon_x} = \sqrt{(1.70)(2.0\times 10^{-6})} = 1.844\times 10^{-3} \text{ m} = 0.1844 \text{ cm} , \\ \theta &= \sqrt{\gamma_x \epsilon_x} = \sqrt{(0.59412)(2.0\times 10^{-6})} = 1.900\times 10^{-3}\text{radian} = 1.900\text{mr} , \\ r_{21} &= -\frac{\alpha_x}{\sqrt{\beta_x \gamma_x}} = -\frac{0.100}{\sqrt{1.7(0.59412)}} = -0.0995 . \end{aligned}$$

The vertical Twiss parameters are identical to those in the horizontal plane. Thus the TRANSPORT input parameters in vertical plane are

$$y = 0.1844 \text{ cm}, \qquad \theta = 1.900\text{mr}, \qquad \text{and } r_{43} = -0.0995 .$$

A value of α_x (α_y) means that there is a waist in the horizontal (vertical) plane. The corresponding conditions in TRANSPORT notation are $r_{21} = 0$ and $r_{43} = 0$. Thus for the assumed initial conditions beam extracted from the accelerator almost is at a double waist.

3. Details of the beamline design

3.1 Distance measurements

We have measured the distance from the east wall of the accelerator vault to the cross-over point of the last dipole of the ISAC I to ISAC II transfer line to be 129.5 ft or 39.472 m[4]. The sketch ISK0186D on the wall of the accelerator vault gives the distance from the point $(z, x) = (0 \text{ m}, 19.000 \text{ m})$ to the cross-over point as 482.89 inches or 12.291 m. The coordinates of the cross-over point are then $(z, x) = (12.291 \text{ m}, 19.000 \text{ m})$. Thus the coordinates of the wall are $(z, x) = (51.763 \text{ m}, 19.000 \text{ m})$. Using the coordinate $(z, x) = (26.101 \text{ m}, 19.000 \text{ m})$ of §2.1 as the exit of the medium beta cavity, we find that the distance from there to the end wall is (51.763 m − 26.101 m) or 25.662 m.

To transport beam from the exit of the β cavity to the object point of the transport system to the experimental area we use the same technique as used in ref[2]—that is, a four-quadrupole matching system followed by two identical unit sections. This section of the beamline will be called the "front-end" throughout this report.

3.2 Matching sections and unit sections

It is important to understand what is meant in the following by the terms matching section and unit section.

In the context of this report a *matching* section is a section of beamline that converts a beam from a source into one with specified parameters. As used in this report, a matching section transforms beam emerging from the medium β accelerator into a double waist of specified size. Here, specifically, beam from the accelerator is brought to a double waist with a beam size of $x = y = \pm 1$ mm.

A *unit* section on the other hand exactly reproduces the object at its image position. Depending on the design of the section the image may be upright or inverted. The simple four-quadrupole unit section used here in the front-end produces an inverted image in each of the horizontal and vertical planes; the transfer matrix from its object to its image is $-\boldsymbol{I}$. Thus a point on the object with spatial coordinates $\boldsymbol{x}_o = (x_o, \theta_o, y_o, \phi_o)$ is transformed to the point on the image with the coordinates $\boldsymbol{x}_i = (-x_i, -\theta_i, -y_i, -\phi_i)$.

Consequently, if the front-end is operated in a matching mode the double waist is reproduced at its exit. Because each of the two following unit sections invert its object, the image of the waist will be upright. However, the *overall* transfer matrix from object to image will *not* be $+\boldsymbol{I}$ because of that of the matching section is not unity. The four beamlines of ref[1] have been designed assuming a double waist at their object point. The addition of a matching section upstream of their object point does not affect their optics. Again, however, the overall transfer matrix from accelerator exit to target will not be a unit matrix.

On the other hand, if the front-end is run as a unit section it is the beam that exits the accelerator that is transported to its exit. In this case, because there are three $-\boldsymbol{I}$ sections the image there will be exactly inverted. Further, the overall transfer matrix from object to image will be exactly $-\boldsymbol{I}$. If the transfer matrix of the downstream beamline is itself $\pm\boldsymbol{I}$, the overall transfer matrix from the accelerator exit to the target will be $\mp\boldsymbol{I}$. The beam size and shape at the target, however, will a replication of the beam extracted from the accelerator.

3.3 The matching section

As in ref[1)] we assume that type L2 quadrupoles are used throughout this beamline. We also use a section of the type $LQQLLQQL$, where L represents a drift space of length L and Q represents a quadrupole. We use this configuration because it can be operated either as a matching system or as a unit section.

The length of the matching section of ref[2)] appears to be 4 m. We have chosen to use a matching section of length 5 m. The system chosen here has $L = 0.825$ m, an effective length of a quadrupole of 0.325 m, and a separation of 0.200 m between the quadrupoles of a doublet.

For use as a matching section all quadrupoles are allowed to vary independently in order to meet the matching requirements. In the case considered here, those requirements were a double waist with a beam size of ± 1 mm in each of the horizontal and vertical planes.

When operating as a unit section the quadrupoles are tuned in alternating polarity to identical (absolute) values of gradient.

3.4 The unit sections

For these sections we also use a $LQQLLQQL$ configuration. From ref[1)] the distance from the object point of the system to the wall is found to be 3.47 m. Given that the length of the matching section has been taken as 5.00 m, the total length of each unit section is

$$\text{total length of one unit section} = \frac{25.662\ \text{m} - (5.000\ \text{m} + 3.470\ \text{m})}{2} = 8.596\ \text{m}\ .$$

The use of type L2 quadrupoles with a separation of the quadrupoles of a doublet of 0.300 m implies that the drift length L of a unit section is

$$L = \frac{8.596\ \text{m} - 4(0.325\ \text{m}) - 2(0.300\ \text{m})}{4} = 1.674\ \text{m}\ .$$

In our calculations we have used $L = 1.675$ m.

3.5 The beamline from medium β exit to waist 3

Table 1 lists the TRANSPORT input for beam transport between the exit of the medium β system and the object point for beam transport to the experimental hall. The input data given in this table is for operation of this section in a *matching* mode. The matching point is labelled WST1. Beam properties at at this point are imaged at the points WST2 and WST3 by the two unit sections.

Figure 1 shows the beam envelopes along the beamline for operation in a matching mode.

As was noted above, the section of beamline from the medium β exit to the point labelled WST1 can also be operated as a unit section. In this case the first four quadrupoles are powered equally and the input for the first four quadrupoles replaced by the following.

5.00	Q1	0.32500	−154.38769	100.00000;
5.00	Q2	0.32500	154.38769	100.00000;
5.00	Q3	0.32500	−154.38769	100.00000;
5.00	Q4	0.32500	154.38769	100.00000;

There are no changes to the setting of any of the other quadrupoles.

When operated in this mode there is a true unit transformation from the exit of the medium beta cavities to the target locations TGT1 and TGT3. Here it is assumed that the downstream optics are those prescribed in ref[1)].

Figure 2 shows the beam profiles in this "front-end" section when it is operated as a unit section.

4. The complete beamline

The full beam-transport configuration to the four target locations proposed in ref[1)] is shown in figure 3. In that figure the locations labelled W1, W2, and W3 are the locations denoted WST1, WST2, and WST3 in table 1.

Figures 4-7 show the beam profiles along each of the four beamlines. In these figures the first four quadrupoles are run in the matching mode. No changes have been made to the proposed beamlines of [1)].

When the first four quadrupoles are operated as a unit section we get the beam profiles shown in figures 8 and 9. Only beam transport to TGT1 and TGT3 has been considered in this mode because they are the only beamlines that are themselves unit sections.

It is interesting to note that when the front-end is run as a unit section the beam envelopes are smaller than when the front-end is run as a matching section. This is clear from a comparison of figure 4 with figure 8 and of figure 6 with figure 9.

The downside of operating the system as a unit section is that the beam parameters at the exit of medium β cavities are reproduced at the targets. In this case, although there is almost a double waist at the targets, the beam size there is (roughly) doubled. This difference in beam size and transport parameters is illustrated in table 2. There the beam parameters and overall transfer matrices at targets TGT1 and TGT3 are compared for the two operational cases.

5. Discussion

This report has presented an updated design for beam transport from the exit of the medium β cavities to the ISAC-II experimental area. Here the proposed beam transport of [1)] has been combined with a simple matching section and two unit sections. It is noted that this front-end section can also be run as a unit section.

References

1. G. M. Stinson, *A revision of the beam transport to the* ISAC-II *experimental area*, TRIUMF report TRI-DNA-04-1, January, 2004.

2. R. E. Laxdal and M. Pasini, *ISAC-II Optics Specifications*, TRIUMF report TRI-DN-01-xx, March, 2002.

3. R. E. Laxdal, *Private communication*, TRIUMF, February, 2004.

4. A. Richardson and G. M. Stinson, TRIUMF, January, 2004.

Table 1

TRANSPORT input for transport from medium beta to experimental hall object point

'Transport from medium beta to experimental hall object point '					
0					
13.		12.00000;			
16.00	G/2	5.00000	2.50000;		
16.00	K1	7.00000	0.45000;		
16.00	K2	8.00000	2.80000;		
1.000000	BEAM	0.10000	2.00000	0.10000	2.00000
		0.00000	0.10000	0.93000;	
12.	CORR	−0.09950	0.00000	0.00000	0.00000
		0.00000	−0.09950	0.00000	0.00000
		0.00000	0.00000	0.00000	0.00000
		0.00000	0.00000	0.00000;	
3.0		0.82500;			
5.00	Q1	0.32500	−190.21381	100.00000;	
3.0		0.30000;			
5.00	Q2	0.32500	165.28305	100.00000;	
3.0	MID1	0.82500;			
3.0		0.82500;			
5.00	Q3	0.32500	−184.78889	100.00000;	
3.0		0.30000;			
5.00	Q4	0.32500	227.95246	100.00000;	
3.0	WST1	0.82500;			
3.0		1.67500;			
5.00	Q5	0.32500	99.80433	100.00000;	
3.0		0.30000;			
5.00	Q6	0.32500	−99.80433	100.00000;	
3.0	MID2	1.67500;			
3.0		1.67500;			
5.00	Q7	0.32500	99.80433	100.00000;	
3.0		0.30000;			
5.00	Q8	0.32500	−99.80433	100.00000;	
3.0	WST2	1.67500;			
3.0		1.67500;			
5.00	Q9	0.32500	99.80433	100.00000;	
3.0		0.30000;			
5.00	Q10	0.32500	−99.80433	100.00000;	
3.0	MID3	1.67500;			
3.0		1.67500;			
5.00	Q11	0.32500	99.80433	100.00000;	
3.0		0.30000;			
5.00	Q12	0.32500	−99.80433	100.00000;	
3.0	WST3	1.67500;			
SENTINEL					
SENTINEL					

Table 2

Predicted beam sizes and overall transfer matrices at TGT1 and TGT2
in the matching and unit section modes of operation

Parameter	TGT1		TGT3	
	Matching	Unit section	Matching	Unit section
$\pm x$ (cm)	0.100	0.184	0.100	0.184
$\pm\theta$ (mr)	2.000	1.090	2.000	1.090
$\pm y$ (cm)	0.100	0.184	0.100	0.184
$\pm\phi$ (mr)	2.000	1.090	2.000	1.090
R_{11} (cm/cm)	−0.4682	−1.0000	−0.4703	−1.0000
R_{12} (cm/mr)	−0.0549	−0.0004	−0.0543	0.0000
R_{16} (cm/%)	0.0000	0.0000	0.0000	0.0000
R_{21} (mr/cm)	5.5108	−0.0003	5.5111	0.0000
R_{22} (mr/mr)	−1.4903	−1.0000	−1.4902	−1.0000
R_{26} (mr/%)	−0.0003	−0.0003	0.0000	−0.0003
R_{33} (cm/cm)	0.3558	1.0000	−0.3568	−1.0000
R_{34} (cm/mr)	0.0755	0.0001	−0.0754	0.0000
R_{43} (mr/cm)	−8.2416	−0.0001	8.2416	0.0000
R_{44} (mr/mr)	1.0622	1.0000	−1.0622	−1.0000

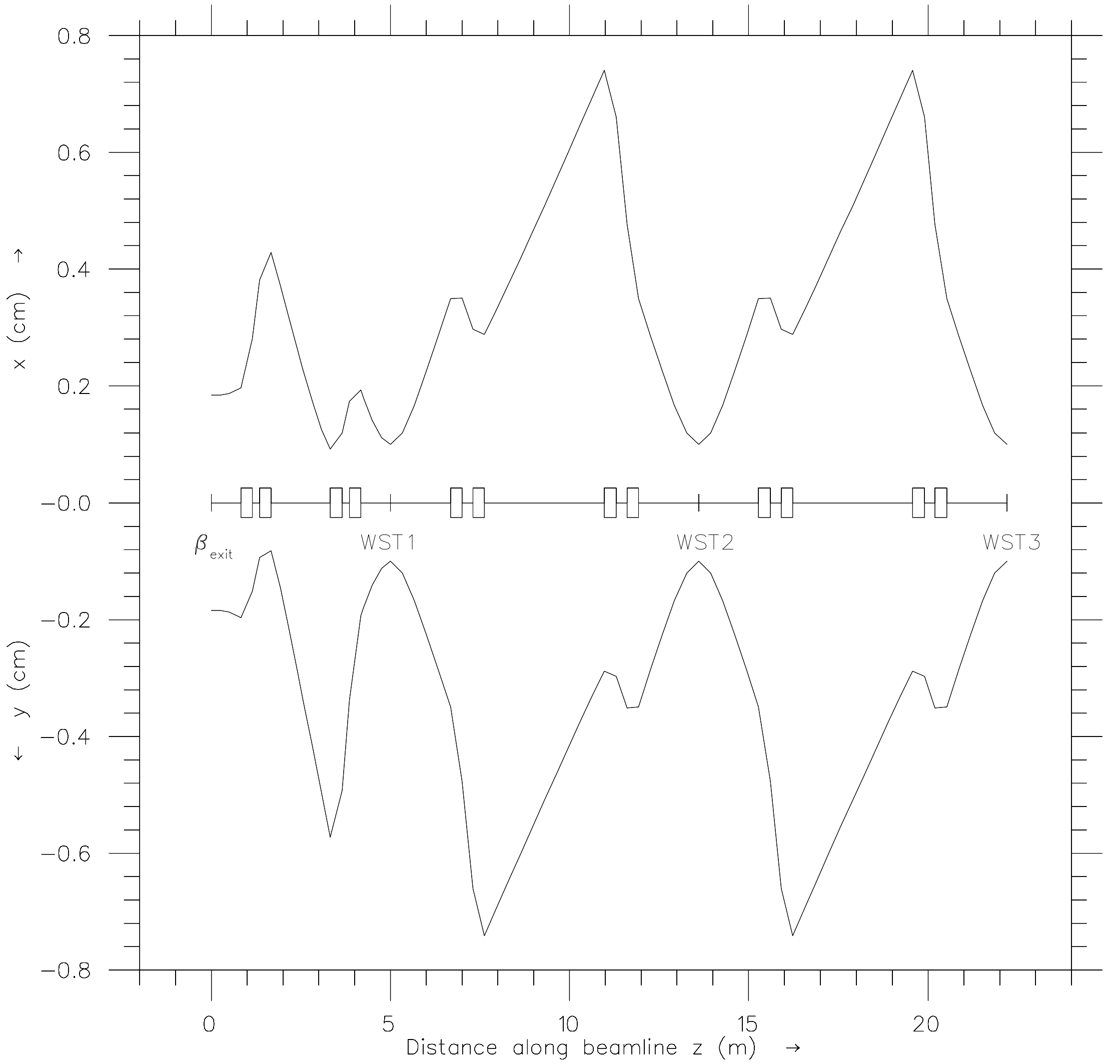

Fig. 1. Beam profiles in the front-end operating as a matching section.

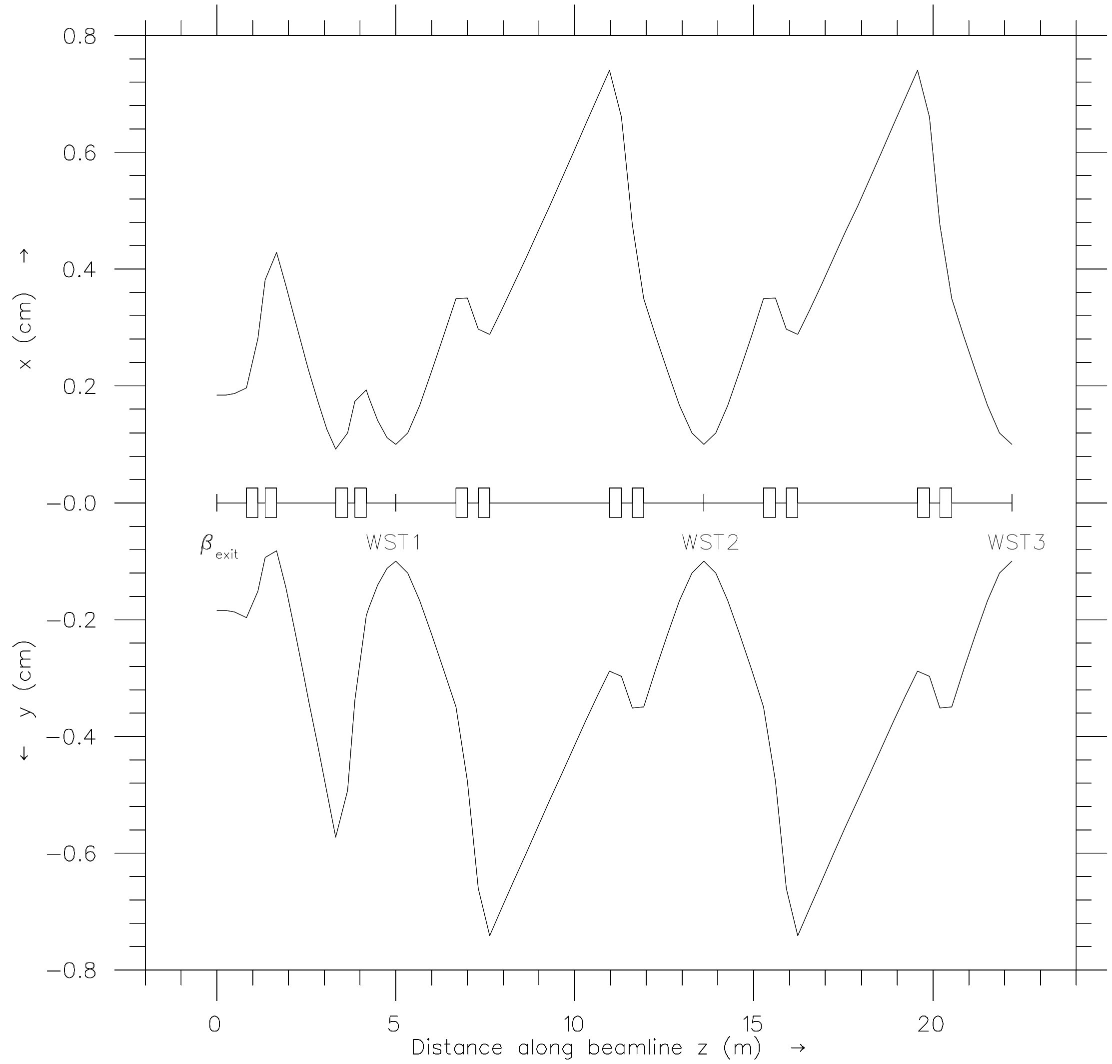

Fig. 2. Beam profiles in the front-end operating as a unit section.

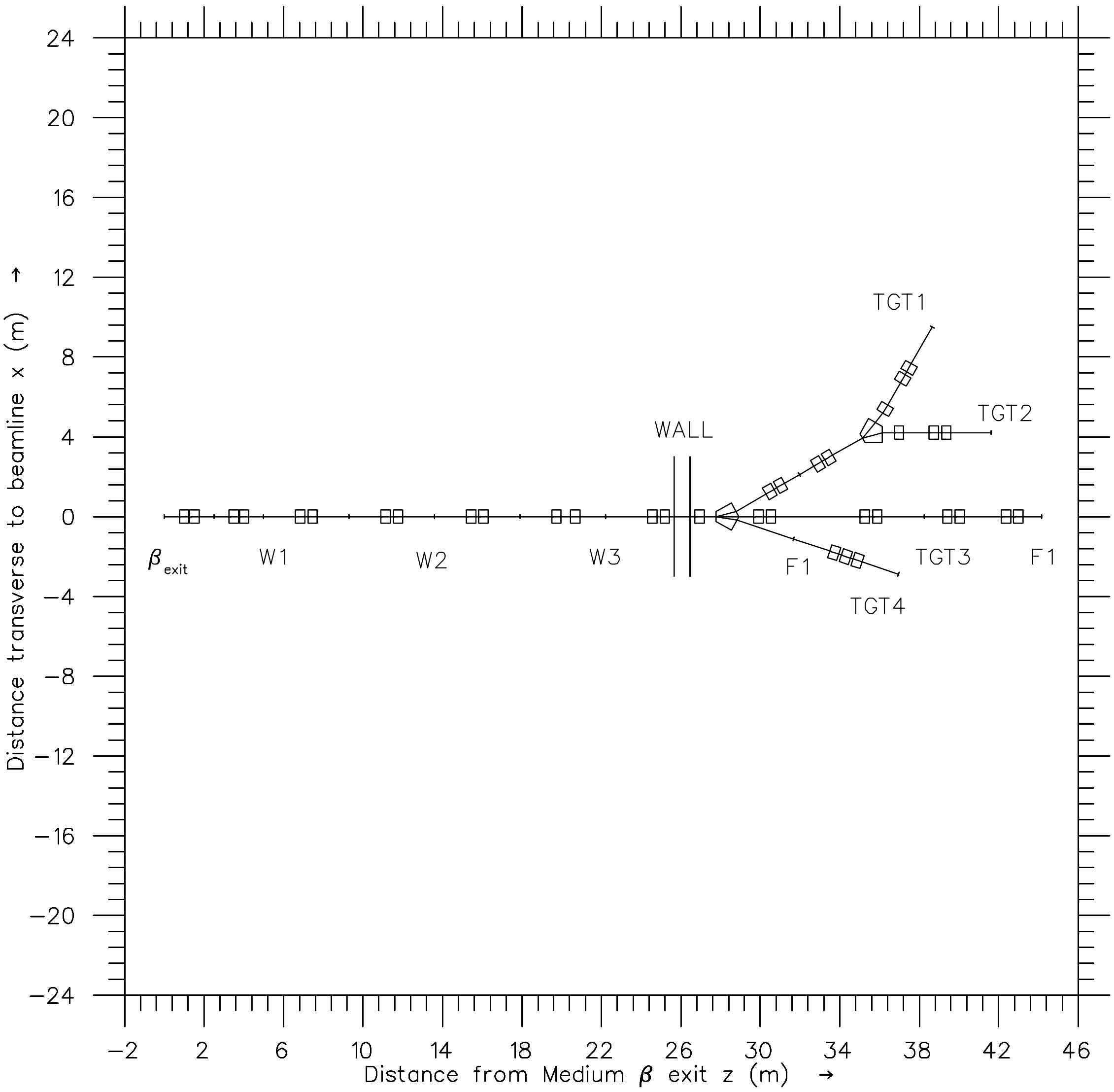

Fig. 3. The proposed beamline configuration for beam delivery to the ISAC-II experimental hall.

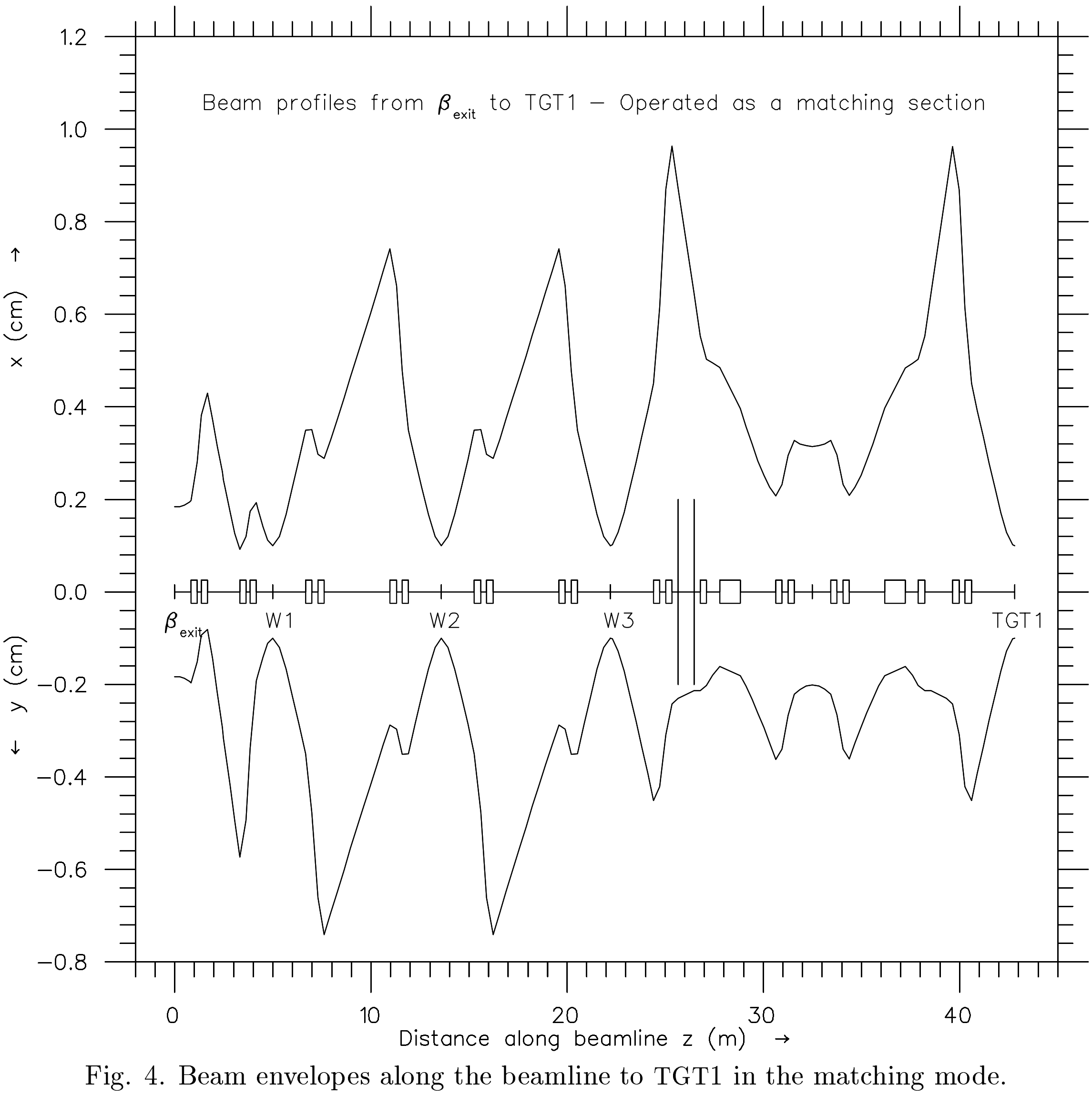

Fig. 4. Beam envelopes along the beamline to TGT1 in the matching mode.

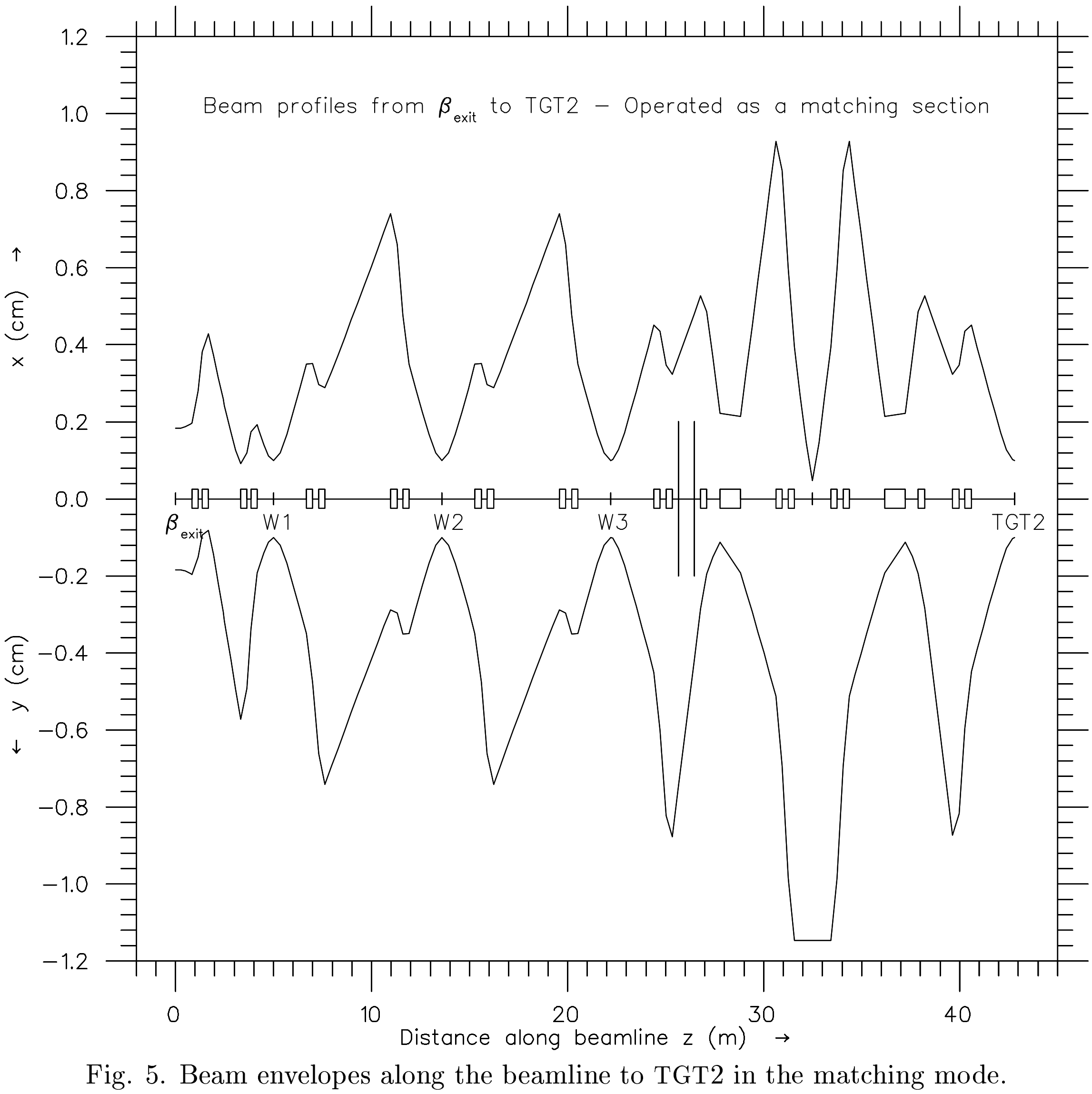

Fig. 5. Beam envelopes along the beamline to TGT2 in the matching mode.

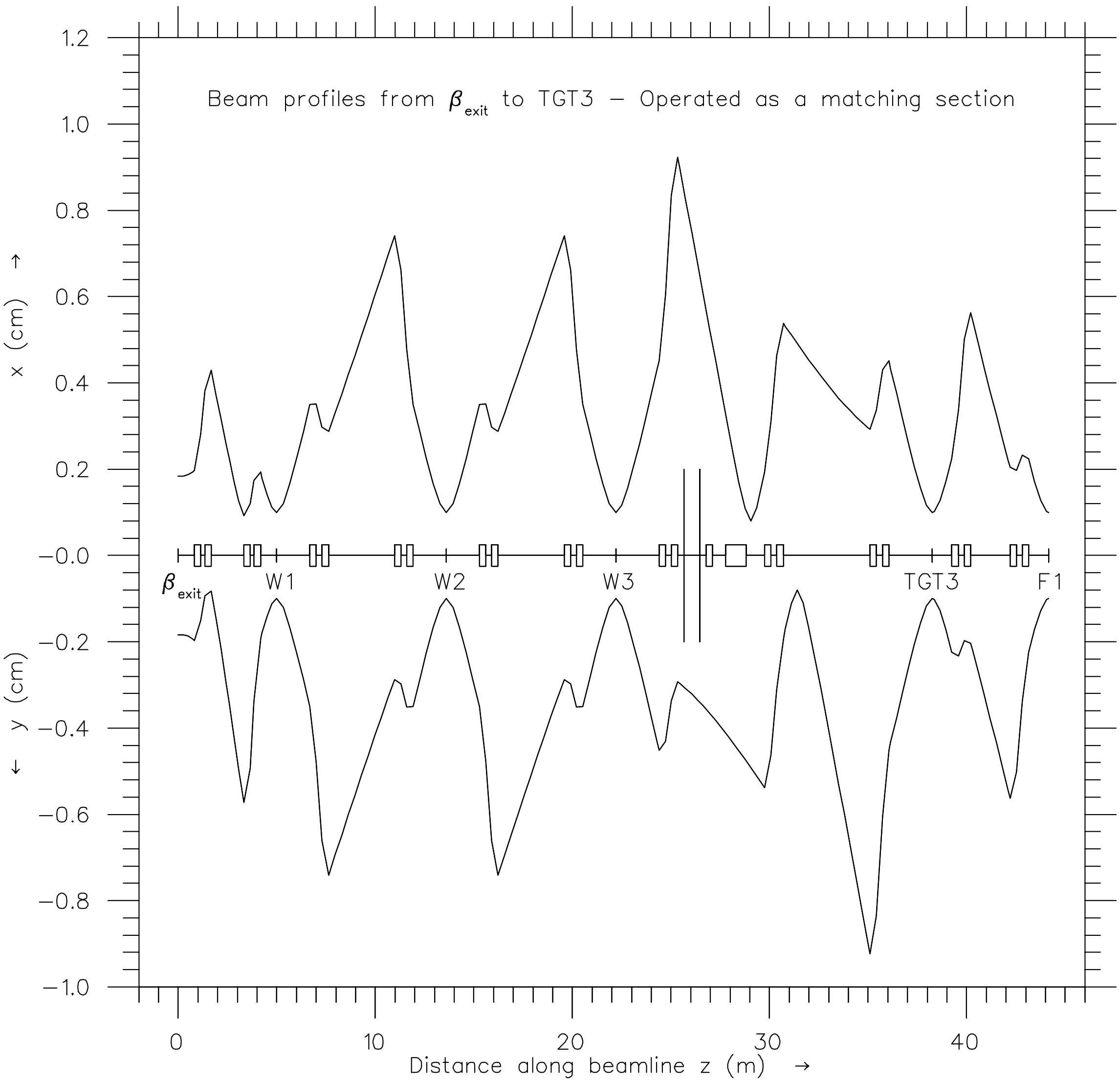

Fig. 6. Beam envelopes along the beamline to TGT3 in the matching mode.

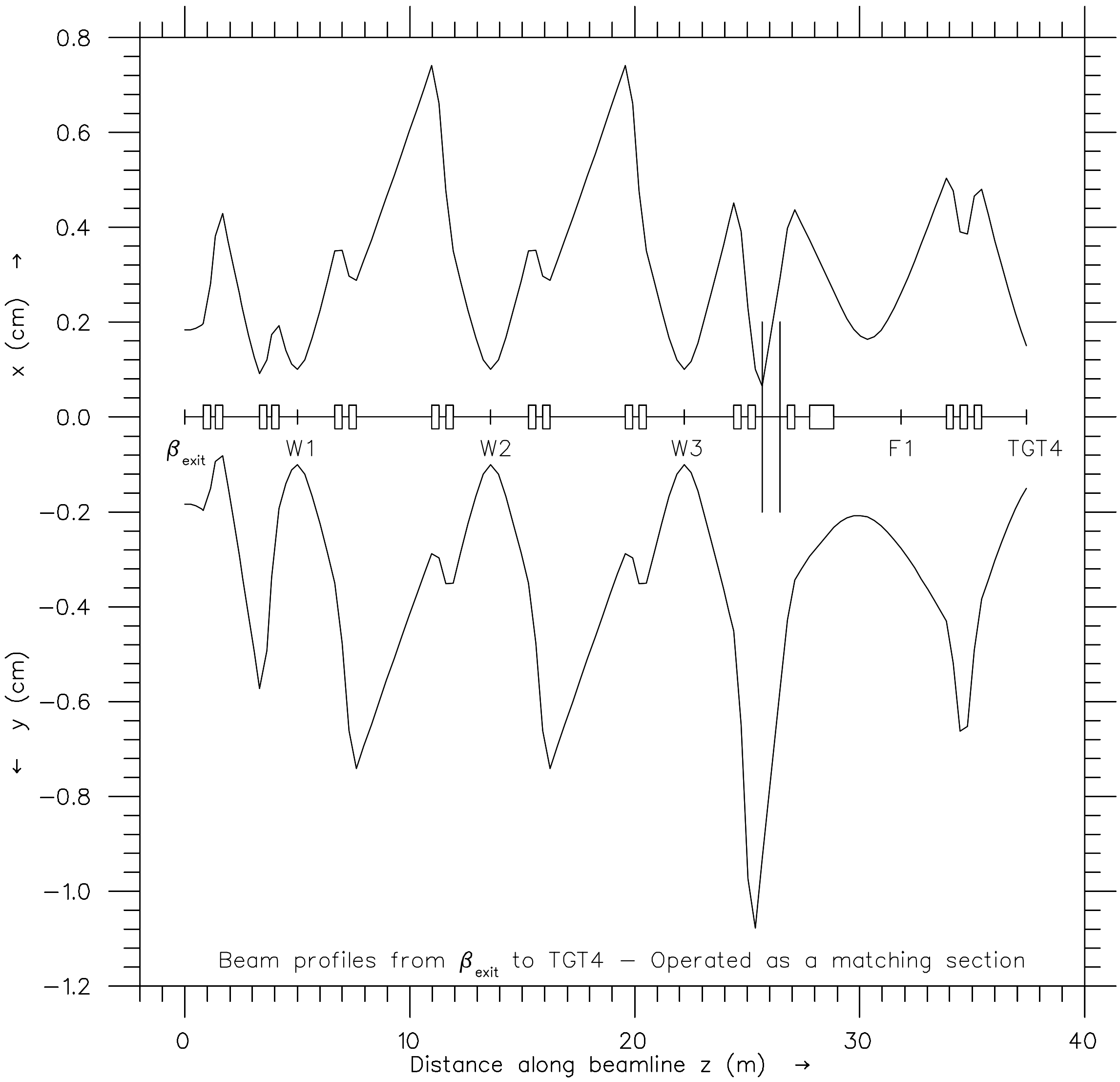

Fig. 7. Beam envelopes along the beamline to TGT4 in the matching mode.

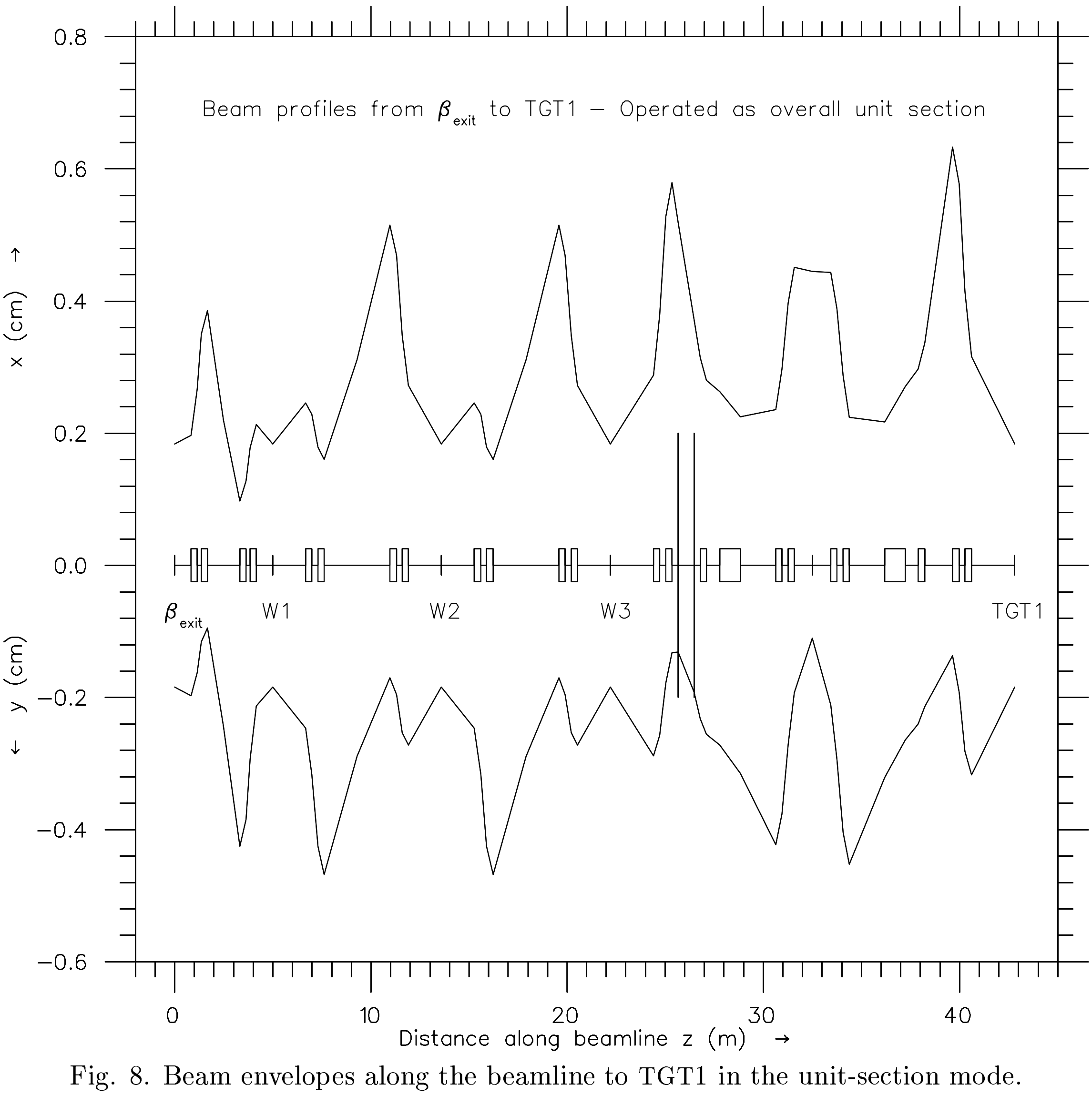

Fig. 8. Beam envelopes along the beamline to TGT1 in the unit-section mode.

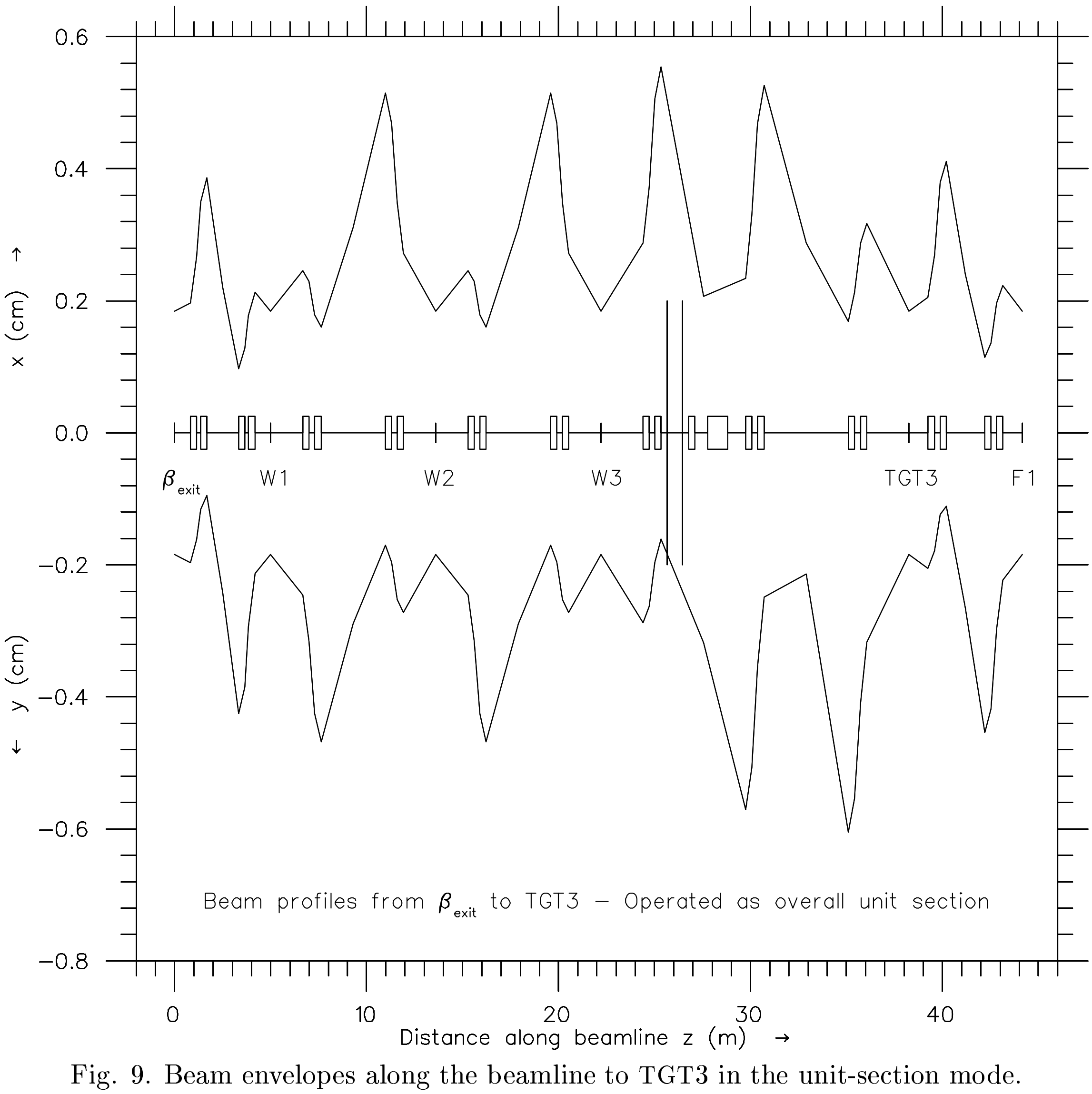

Fig. 9. Beam envelopes along the beamline to TGT3 in the unit-section mode.